

# Determination of the Nuclear Matrix Elements in the 2.31-Mev $\beta$ Transition of $\text{Sb}^{124}$ through Measurement of the $\beta$ - $\gamma$ (Circularly Polarized) Angular Correlation\*†

P. ALEXANDER AND R. M. STEFFEN  
Department of Physics, Purdue University, Lafayette, Indiana  
(Received May 16, 1961)

The degree of circular polarization ( $P_c$ ) of the 0.603-Mev gamma radiation following the first-forbidden  $\beta$  transition from the  $3^-$  ground state of  $\text{Sb}^{124}$  to the  $2^+$  first excited state of  $\text{Te}^{124}$  was measured. The dependence of  $P_c$  on the angle  $\theta_{\beta\gamma}$  between the  $\beta$  and  $\gamma$  momentum vectors was determined. Representative values of  $P_c(\theta_{\beta\gamma})$  at some of the angles  $\theta_{\beta\gamma}$  measured are  $P_c = 0.061 \pm 0.071$  at  $\theta_{\beta\gamma} = 105^\circ$ ,  $P_c = 0.349 \pm 0.083$  at  $\theta_{\beta\gamma} = 122^\circ$ ,  $P_c = 0.604 \pm 0.054$  at  $\theta_{\beta\gamma} = 152^\circ$ , and  $P_c = 0.373 \pm 0.071$  at  $\theta_{\beta\gamma} = 168^\circ$ . These values were obtained at  $\bar{W} = 4.6$ . The 2.31-Mev  $\beta$  transition of  $\text{Sb}^{124}$  is known to contain an unusually large contribution from the  $fB_{ij}$  matrix element (which describes the component of the lepton field carrying away two units of angular

momentum). The measured  $\beta$ - $\gamma$  circular-polarization correlation data, the  $\beta$ - $\gamma$  directional correlation, and spectral shape data were analyzed by use of a digital computer on the basis of the Kotani parameters  $Y$ ,  $x$ ,  $u$ , and  $z$ . A somewhat generous summary of the final data may be given by  $Y = 0.6 \pm 0.3$ ,  $x = -0.055 \pm 0.105$ ,  $u = -0.060 \pm 0.140$ ,  $z = 1$ . Values of the nuclear matrix elements are extracted from the  $ft$  value of the 2.31-Mev  $\beta$  transition and the measured Kotani parameters, yielding  $fB_{ij}/R = \pm(1.4 \pm 0.2) \times 10^{-2}$ ,  $f\mathbf{r}/R = \mp(9.3 \pm 17.6) \times 10^{-4}$ ,  $f\mathbf{i}\sigma \times \mathbf{r}/R = \mp(8.1 \pm 18.9) \times 10^{-4}$ ,  $f\mathbf{i}\alpha = \pm(1.6 \pm 0.8) \times 10^{-4}$ .  $R$  is the nuclear radius of  $\text{Sb}^{124}$  in units of  $\hbar/mc$ . The significance of suppression of the matrix elements other than  $fB_{ij}$  is discussed.

## 1. INTRODUCTION

A NUMBER of facts indicate an unusually large contribution of the  $fB_{ij}$  nuclear matrix element to the first-forbidden ( $\Delta I = 1$ )  $\beta_1$  spectrum of  $\text{Sb}^{124}$  with maximum energy 2.31 Mev. The shape of this spectrum deviates strongly from the statistical shape.<sup>1</sup> The energy dependence of the directional-correlation anisotropy factor also requires a large contribution from the  $fB_{ij}$  matrix element.<sup>2</sup> In addition the  $ft$  value of this  $\beta$  transition is extraordinarily large ( $\log ft = 10.6$ ) for a nonunique first-forbidden transition. All these experimental facts indicate either a reduction in, or a mutual cancellation of, the "normal" matrix elements ( $f\mathbf{i}\alpha$ ,  $f\mathbf{r}$ , and  $f\mathbf{i}\sigma \times \mathbf{r}$ ) of tensor rank  $\lambda = 1$ .

Comparison of the energy dependence of the experimentally determined shape factor and of the directional

correlation anisotropy factor with the theoretical predictions, gives important information as to the relative magnitude of the nuclear matrix elements which contribute to the  $\beta$  decay. Nevertheless, the use of these experimental data alone is not sufficient to permit an unique determination of all the matrix elements involved in the  $\text{Sb}^{124}$   $\beta_1$  transition. For this determination an additional set of data is necessary. In particular, the measurement of the angular distribution  $P_c(\theta)$  of the circularly polarized  $\gamma$  radiation with respect to the momentum direction of the preceding  $\beta$  particle furnishes this additional information. Measurement of  $P_c(\theta)$  also provides a very sensitive tool for the determination of the relative contribution of the  $fB_{ij}$  component to the  $\beta$  transition.

The  $\beta$ - $\gamma$  circular polarization correlation involving a first-forbidden  $\beta$  transition is of the form<sup>3-6</sup>:

$$W_{\beta\gamma}(\theta) = A_0(W) + \tau A_1(W)P_1(\cos\theta) + A_2(W)P_2(\cos\theta) + \tau A_3(W)P_3(\cos\theta), \quad (1)$$

where  $\tau$  characterizes the circular polarization of the  $\gamma$ -radiation:  $\tau = +1$  ( $-1$ ) for right (left) circularly polarized  $\gamma$  radiation. The coefficient of the  $P_3(\cos\theta)$  term is different from zero, *only* if the  $fB_{ij}$  contribution to the  $\beta$  transition is nonvanishing. Thus the observation of the mere presence of this term indicates a non-negligible  $fB_{ij}$  matrix element.

If the degree of circular polarization  $P_c(\theta)$  is defined as

$$P_c(\theta) = (N^+ - N^-)/(N^+ + N^-), \quad (2)$$

where  $N^+$  ( $N^-$ ) is the intensity of the right (left) circularly-polarized  $\gamma$  radiation, then the degree of circular polarization  $P_c(\theta)$ , observed at an angle  $\theta$  with respect

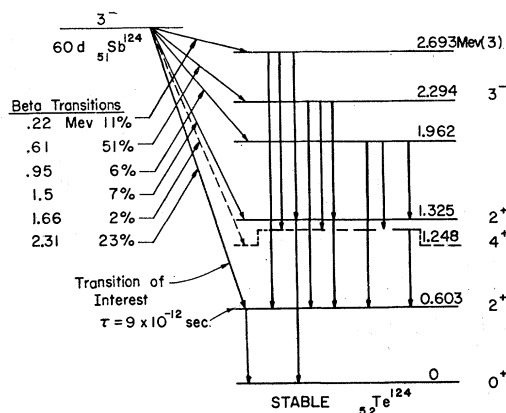


FIG. 1. Decay scheme of  $\text{Sb}^{124}$ .

\* Supported by the U. S. Atomic Energy Commission.

† The work reported in this paper is based on a dissertation submitted by P. Alexander to the Graduate School of Purdue University in partial fulfillment of the requirements for the degree of Doctor of Philosophy.

<sup>1</sup> L. M. Langer and D. R. Smith, Phys. Rev. **119**, 1308 (1960).

<sup>2</sup> R. M. Steffen, preceding paper [Phys. Rev. **124**, 145 (1961)].

<sup>3</sup> K. Alder, B. Stech, and A. Winther, Phys. Rev. **107**, 728 (1957).

<sup>4</sup> M. Morita and R. S. Morita, Phys. Rev. **109**, 2048 (1958).

<sup>5</sup> T. Kotani, Phys. Rev. **114**, 795 (1959).

<sup>6</sup> T. Kotani and M. Ross, Progr. Theoret. Phys. (Kyoto) **20**, 643 (1958).

to the momentum vector of the preceding  $\beta$  particle, is given by

$$P_e(\theta) = \frac{A_1(W)P_1(\cos\theta) + A_3(W)P_3(\cos\theta)}{A_0(W) + A_2(W)P_2(\cos\theta)}. \quad (3)$$

The coefficients  $A_i(W)$  are given in a convenient form by Kotani.<sup>5</sup>  $A_0(W)$  is identical with the  $\beta$ -spectrum shape correction factor  $C(W)$ . In a first-forbidden beta transition, with maximum energy  $W_0$  for which  $\Delta I = \pm 1$  and  $I_0 + I_1 \geq 2$ , we may express  $A_0(W)$  as

$$\begin{aligned} A_0(W) = C(W) = (1/12)[(W_0 - W)^2 + \lambda_1(W^2 - 1)]z^2 + Y^2 \\ + \left[ \frac{2}{3W} - \frac{2W_0}{3} \right] xY + \left[ \frac{2}{3W} - \frac{4}{3}W + \frac{2W_0}{3} \right] uY \\ + \left[ \frac{W_0^2}{3} - \frac{1}{9} - \frac{4WW_0}{9} - \frac{2}{9} \frac{W_0}{W} + \frac{4}{9}W^2 \right] x^2 \\ + \left[ \frac{W_0^2}{6} - \frac{7}{18} - \frac{5}{9}WW_0 + \frac{2}{9} \frac{W_0}{W} + \frac{5}{9}W^2 \right] u^2, \quad (4) \end{aligned}$$

where  $Y$ ,  $u$ ,  $x$ , and  $z$  are the matrix element parameters<sup>5</sup>

$$\begin{aligned} x &= -(1/s)C_V \int \mathbf{r}, \\ u &= (1/s)C_A \int i\boldsymbol{\sigma} \times \mathbf{r}, \\ z &= (1/s)C_A \int B_{ij}, \\ Y &= -(1/s)C_V \int i\boldsymbol{\alpha} - \xi(u+x); \quad \xi = \alpha Z/2R. \end{aligned} \quad (5)$$

The parameters introduced above are pure numbers; they represent the contributions of the various matrix elements as compared to a standard matrix element ( $s$ ) for which we may choose any nonvanishing matrix element contributing to the  $\beta$  transition. These parameters are convenient to use, since the shape factor and the angular correlation coefficients depend only on the ratios of matrix elements. For the computation of the absolute transition probability,  $|s|^2$  can be taken out as a common factor. Thus  $|s|^2$  is determined by the  $ft$  value of the transition

$$|s|^2 = \frac{\pi^3 \ln 2}{f_e t}, \quad (6)$$

where

$$f_e = \int_1^{W_0} F_0(Z, W) p W (W_0 - W)^2 C(W) dW, \quad (7)$$

and  $t$  is the half-life of the  $\beta$  transition.<sup>7</sup>  $F_0(Z, W)$  is the Fermi function. In the evaluation of the  $\text{Sb}^{124}$  data we chose  $C_A \int B_{ij}$  as the standard matrix element

$$s = C_A \int B_{ij}, \quad \text{or equivalently} \quad z = 1,$$

since there is good evidence that  $C_A \int B_{ij} \neq 0$ , whereas any other matrix element might possibly vanish.<sup>2</sup> In the following theoretical expressions  $z$  is not replaced by 1 in order to keep the equations as general as possible and also to make apparent the terms which arise from the presence of the  $\int B_{ij}$  component.

The directional-correlation anisotropy coefficient  $A_2(W)$  for a  $3^-(\beta^-) \rightarrow 2^+(\gamma, E2) \rightarrow 0^+$   $\beta$ - $\gamma$  cascade is given by the following expressions<sup>5</sup>:

$$\begin{aligned} A_2(W) = \frac{-1}{252C(W)} \frac{p^2}{W} [6\lambda_1 W z^2 + 36\lambda_2 zY \\ - (12\lambda_2 W_0 - 12W)xz - (30W - 12\lambda_2 W_0)uz \\ + 24\lambda_3 xY - 12\lambda_3 uY - (8\lambda_2 W_0 + 4W)x^2 \\ - (4\lambda_2 W_0 - 7W)u^2 - (12W - 12\lambda_2 W_0)ux]. \quad (8) \end{aligned}$$

The coefficients  $A_1(W)$  and  $A_3(W)$  appearing in the expression for the  $\beta$ - $\gamma$  circular polarization correlation of the first-forbidden  $3^-(\beta^-) \rightarrow 2^+(\gamma, E2) \rightarrow 0^+$  cascade are rather complex<sup>5</sup>:

$$\begin{aligned} A_1(W) = \frac{p}{W} \frac{1}{180} [-60Y^2 - 60\lambda_4 W Y z \\ + 4(5W_0^2 + 6W^2 - 5WW_0 - 6)xz \\ + 2(5W_0^2 + 24W^2 - 20WW_0 - 9)uz \\ + 20(5W - 2W_0)uY + 40(W_0 - W)xY \\ + 20(W_0^2 - 3WW_0 + 2W^2)ux \\ + 5(3 - W_0^2 + 6WW_0 - 8W^2)u^2], \quad (9) \end{aligned}$$

and

$$A_3 = \frac{p^3}{W} \left[ \frac{1}{28} \lambda_1 z^2 + \frac{2}{35} xz - \frac{1}{35} uz \right]. \quad (10)$$

The coefficients  $\lambda_i$ , which are of order unity, contain the effects of the Coulomb field of the nucleus on the electron wave functions. These effects are of order  $\alpha Z W/p$ . For  $i=1$  and  $i=2$  the values of  $\lambda_i$  are tabulated.<sup>8</sup> The expression for  $\lambda_4$  is given in Kotani's paper.<sup>5</sup>

Equations (4)–(10) will be used in this work to ex-

<sup>7</sup> Usually  $t$  is expressed in seconds, while the function  $f_e$  is computed in units  $m_0 = c = 1$ . Consequently, the  $f_e t$  values are usually given in the hybrid units  $m_0 = c = 1$ ,  $t$  in seconds. In applying Eq. (6),  $f_e t$  is most conveniently expressed in units  $m_0 = c = \hbar = 1$ ; thus  $t$  must then be expressed in units  $\hbar/m_0 c^2$ . In this system the unit of time corresponds to  $1.3 \times 10^{-21}$  sec.

<sup>8</sup> T. Kotani and M. Ross, Phys. Rev. **113**, 622 (1959).

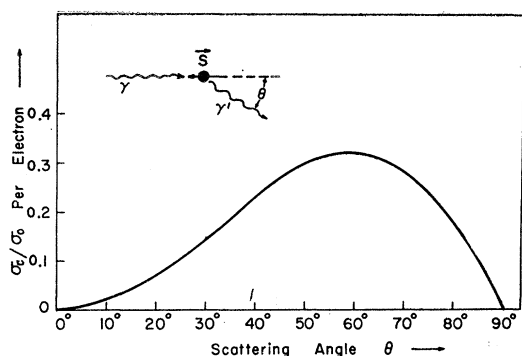


FIG. 2. Ratio of polarization-sensitive part of the Compton scattering cross section ( $\sigma_c$ ) to polarization-insensitive part of the Compton cross section ( $\sigma_0$ ) for 0.603-Mev gamma rays scattered on polarized electrons with spin  $S$ .

tract the values of the nuclear matrix elements which are consistent (a) with the observed shape factor of the  $\text{Sb}^{124}$   $\beta$  spectrum (Langer *et al.*),<sup>1</sup> (b) with the measured  $\beta$ - $\gamma$  directional correlation (Steffen,<sup>2</sup> preceding paper), and (c) with the  $\beta$ - $\gamma$  circular polarization correlation whose determination is described in this paper.

## 2. EXPERIMENTAL

### A. Circular Polarization Analyzer

The degree of circular polarization of the 0.603-Mev  $\gamma$  radiation of  $\text{Sb}^{124}$  (Fig. 1) was determined by the method of Compton scattering on polarized electrons.<sup>9-10</sup> This mode of detection is based on the fact that we may write the Compton scattering cross section as the sum of a polarization-insensitive term ( $\sigma_0$ ) and a polarization-sensitive term ( $\sigma_c$ ) (see Fig. 2). A magnetized hollow iron cylinder which formed part of a large electromagnet, provided the ensemble of polarized electrons. Figure 3 shows a schematic diagram of the circular-polarization analyzer which was used in the  $\beta$ - $\gamma$  circular-polarization correlation measurements described in this paper. The circular polarization analyzer is similar to arrangements used by Schopper,<sup>11</sup> Boehm and Wapstra,<sup>12</sup> and Steffen.<sup>13</sup> The geometry was designed to give optimum performance with regard to maximum circular-polarization efficiency  $E(h\nu)$  and minimum angular spread for the 0.603-Mev  $\gamma$  radiation of  $\text{Sb}^{124}$ . The circular polarization efficiency  $E(h\nu)$  of the analyzer is defined by the relation

$$P_c E(h\nu) = (N^+ - N^-) / (N^+ + N^-) = \delta,$$

where  $P_c$  is the degree of circular polarization of gamma radiation emitted by the (point) source and  $N^-$  ( $N^+$ ) is the gamma-counting rate observed with the electron spins pointing toward (away from) the source. The efficiency  $E(h\nu)$  was computed by graphical integration

over the scattering volume exposed to the  $\gamma$  radiation (inner portion of the hollow iron cylinder) and over the  $\text{NaI(Tl)}$  scintillation detector, using the Compton scattering cross-section expressions of Franz<sup>14</sup> and others.<sup>15, 16</sup> The polarization efficiency  $E(h\nu)$  is directly proportional to the fraction ( $f$ ) of electrons in the iron core which are polarized. The method for computing  $f$  has been described previously.<sup>13</sup> The absorption of the  $\gamma$  radiation in the iron scatterer before and after scattering, was considered. Also considered was the effect of  $\gamma$ -ray depolarization (during the scattering process) on absorption in the iron. The variation of the response of the scintillation detector for the different energies of the  $\gamma$  radiation scattered at different angles and in different (nonaxial) planes was taken into account. Plural scattering effects which give an appreciable contribution to the intensity of the scattered radiation, but have only a small influence on the polarization efficiency, were neglected in this calculation.

The degree of circular polarization  $P_c(\theta)$  depends on the angle  $\theta$  between the momentum vector of the preceding  $\beta$  particle and the propagation direction of the gamma radiation [cf. Eq. (3)]. The variation of  $P_c(\theta)$  with  $\theta$  was not taken into account in the computation of  $E(h\nu)$ , since  $P_c(\theta)$  was not known at the beginning of the experiment. This correction which concerns the finite angular acceptance angle of the  $\beta$  and  $\gamma$  radiation will be considered later in the comparison of the theoretical and experimental curves for  $P_c(\theta)$ .

It is important to realize that the average angle  $\bar{\theta}_{\beta\gamma}$  between the momentum vectors of the  $\beta$  and  $\gamma$  radiation differs from the "instrument" angle  $\theta'$ . The latter is defined as the angle between the axes of the  $\beta$  detector and the analyzer magnet. The difference between  $\bar{\theta}_{\beta\gamma}$  and  $\theta'$  is particularly evident at the  $\theta' = 180^\circ$  position which, in one of our geometrical arrangements, corresponds to an average  $\beta$ - $\gamma$  angle  $\bar{\theta}_{\beta\gamma}$  of approximately  $155^\circ$ .

It was found necessary to limit the spread in  $\theta_{\beta\gamma}$  by reducing the aperture of the magnet entry port. This

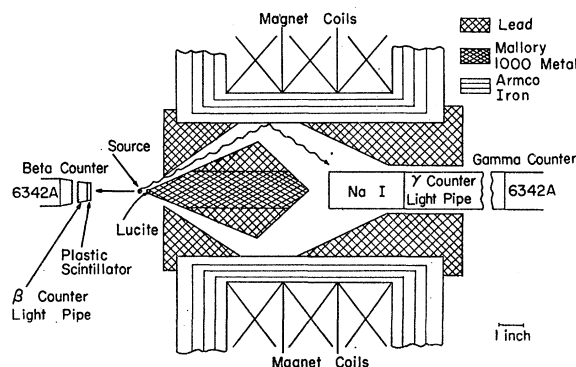


FIG. 3. Polarization analyzer magnet and radiation detectors.

<sup>9</sup> H. A. Tolhoek, *Revs. Modern Phys.* **28**, 277 (1956).

<sup>10</sup> H. Schopper, *Nuclear Instr.* **3**, 158 (1958).

<sup>11</sup> H. Schopper, *Phil. Mag.* **2**, 710 (1957).

<sup>12</sup> F. Boehm and A. H. Wapstra, *Phys. Rev.* **109**, 456 (1958).

<sup>13</sup> R. M. Steffen, *Phys. Rev.* **115**, 980 (1959).

<sup>14</sup> W. Franz, *Ann. Physik*, **33**, 689 (1938).

<sup>15</sup> U. Fano, *J. Opt. Soc. Am.* **39**, 859 (1959).

<sup>16</sup> F. W. Lipps and H. A. Tolhoek, *Physica* **20**, 85 and 395 (1954).

was accomplished by inserting radial lead baffles whose form is shown in the inset of Fig. 4. A rigorous calculation of the relative  $\gamma$ -ray detection probability  $Q(\theta_{\beta\gamma})$  as a function of  $\theta_{\beta\gamma}$  was performed for different apertures by employing a Burroughs electronic digital computer. The results of these calculations are shown in Fig. 4. The average  $\beta$ - $\gamma$  angle  $\bar{\theta}_{\beta\gamma}$  was then determined as a function of the instrument angle  $\theta'$  by graphical integration.

## B. Detectors and Electronics

The  $\beta$ - $\gamma$  circular polarization correlation equipment (Fig. 5) was designed to permit simultaneous measurement of  $P_c(\theta_{\beta\gamma})$  at four different angles  $\theta'$ . The four  $\beta$  detectors were 0.44-in. thick Pilot B plastic scintillator disks mounted via tapered Lucite light pipes on RCA 6342A photomultipliers. The Pilot B disks were covered with aluminum foils of 0.001-in. thickness. The energy resolution of the  $\beta$  detectors was 21% at 0.62 Mev with a 7 in. light pipe. The magnetic shielding of the photomultiplier tubes consisted of several layers of Netic and Co-Netic iron foils surrounded by a Mu-metal shield and a soft iron tube. The  $\gamma$  detector was a NaI(Tl) cylinder 3 in. long, and 1.5 in. in diameter mounted on an RCA 6342A photomultiplier. The energy resolution of the  $\gamma$  detector was 16% at 0.66 Mev with an 8 in. light pipe. In addition to a magnetic shielding similar to the one described above, a compensating coil was placed around the  $\gamma$  photomultiplier. This compensating coil was wired in parallel with the magnet coil.

The electronics (see Fig. 5) was of the usual fast-slow type. The electronic circuits were designed for a high degree of stability rather than for extremely short resolving times. The four fast coincidence circuits were operated with a resolving time of  $\tau = 7 \mu\text{sec}$ .

Figure 6 shows the energy spectrum of the  $\text{Sb}^{124}$  gamma radiation as it was observed in the  $\gamma$  detector after having been scattered in the analyzer magnet

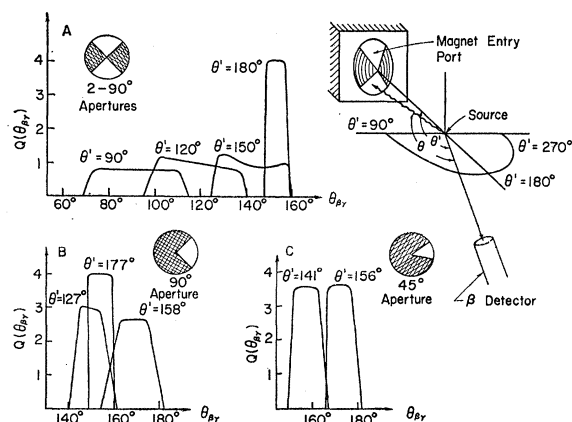


FIG. 4. Relative probability distribution of angles  $\theta_{\beta\gamma}$  as a function of  $\beta$ -detector angle  $\theta'$  (see inset upper right), for magnet baffles A, B, C.

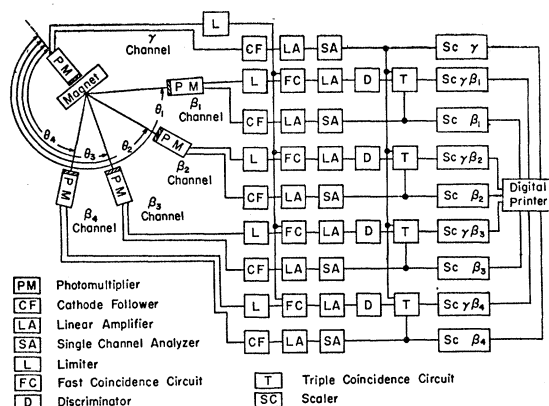


Fig. 5. Block diagram of electronic system for measurement of the beta-gamma circular polarization correlation.

(solid line). For purposes of comparison the spectrum of the  $\text{Sb}^{124}$  gamma radiation observed directly (without scattering) is indicated in the same graph (dotted line). The broad peak in the "scattered" spectrum at about 0.35 Mev corresponds to the 0.603-Mev radiation scattered at an average angle of  $67^\circ$ . The measured energy distribution of the scattered radiation agrees with the energy distribution calculated on the basis of the geometry of the analyzer-detector arrangement. The broad peak at approximately 0.160 Mev is due to radiation scattered from the Pb shielding surrounding the  $\gamma$  detector. The peak at 0.08 Mev is caused by the x radiation from Pb.

## C. Measurements and Results

The  $\text{Sb}^{124}$  was obtained from Oak Ridge National Laboratory in hydrochloric acid solution. The sources were prepared by evaporating to dryness a small drop of the solution on a 0.001-in. Mylar foil.

The four  $\beta$  single-channel analyzers were carefully adjusted by means of a 200-channel analyzer and a precision pulser to accept  $\beta$  particles in the energy range between 1.66 and 2.31 Mev. The 0.624-Mev electron conversion peak of the 0.662-Mev gamma radiation of  $\text{Ba}^{137}$  was used for the energy calibration. The stability of the  $\beta$ -energy selection was frequently checked by means of the 200-channel analyzer.

The single-channel analyzer in the  $\gamma$  channel was set (in a manner similar to the  $\beta$  single-channel analyzers) to accept photons in the energy range from 0.260 to 0.500 Mev, as indicated in Fig. 5.

By integrating the  $\beta$  spectrum of  $\text{Sb}^{124}$  between 1.66 and 2.31 Mev, the average  $\beta$  energy accepted in the  $\beta$ - $\gamma$  circular polarization measurement was determined as 1.84 Mev or  $\bar{W} = 4.6$ .

The coincidence counting rates  $C_{\beta\gamma}'(+)$  and  $C_{\beta\gamma}'(-)$  measured with the magnetic induction in the (+) and (-) direction, were accumulated continuously over a period of more than six months. The magnetic induction was reversed every 20 min in order to minimize

possible drift effects. The data were then corrected for the presence of true  $\gamma$ - $\gamma$  coincidences ( $\approx 3\%$ ) and for chance coincidences ( $\approx 37\%$ ). The high single-count rate made it necessary to include higher-order chance coincidence effects arising from the finite resolving time of the slow triple-coincidence circuit.<sup>17</sup> The coincidence-counting rate for each measuring interval was always divided by the product of the single-counting rates observed in the  $\beta$  and  $\gamma$  detectors over that interval:  $N(\pm) = C_{\beta\gamma}(\pm) / [S_{\beta}(\pm)S_{\gamma}(\pm)]$ , where  $C_{\beta\gamma}$  is the coincidence counting rate corrected for the effects mentioned above.

After applying all the corrections, the quantity  $\delta = (N^+ - N^-) / (N^+ + N^-)$  was computed from the data accumulated at different instrument angles  $\theta'$ . Measurements were made at instrument angles  $\theta' = 90^\circ, 105^\circ, 120^\circ, 130^\circ, 140^\circ, 150^\circ$ , and  $180^\circ$  with lead baffles *A* (see Fig. 4), at angles  $\theta' = 127^\circ, 146^\circ, 158^\circ$ , and  $177^\circ$  with lead baffle *B*, and at angles  $\theta' = 141^\circ, 158^\circ, 208^\circ$ , and  $232^\circ$  with baffle *C*. From the calculated curves of the relative detection probability  $Q(\theta_{\beta\gamma})$ , similar to the ones shown in Fig. 4, the average angle  $\bar{\theta}_{\beta\gamma}$  was obtained. It was then possible to assign an angle  $\bar{\theta}_{\beta\gamma}$  to each instrument angle  $\theta'$  at which  $\delta(\bar{\theta}_{\beta\gamma})$  was measured. The degree of circular polarization  $P_c(\bar{\theta}_{\beta\gamma})$  was computed by employing the relationship  $P_c(\bar{\theta}_{\beta\gamma}) = \delta(\bar{\theta}_{\beta\gamma}) / E$  (0.603 Mev).

The experimental points for  $P_c(\bar{\theta}_{\beta\gamma})$  shown in Fig. 7 are not corrected for the finite angular resolution of the instrument. Shown with the experimental points are horizontal bars which indicate the finite angular resolution of the instrument. The vertical-error bars show the rms statistical error. Analysis of the daily fluctuations in the data recorded at a given angle indicates that these fluctuations are of a statistical nature. It may be noted that our results do not agree with those of

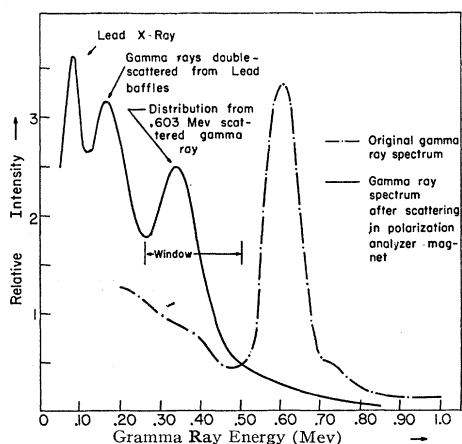


FIG. 6. Part of the gamma ray spectrum of  $\text{Sb}^{124}$ , viewed directly, and observed by the gamma detector after scattering from polarization analyzer magnet.

<sup>17</sup> H. Paul, Nuclear Instr. 9, [131] (1960).

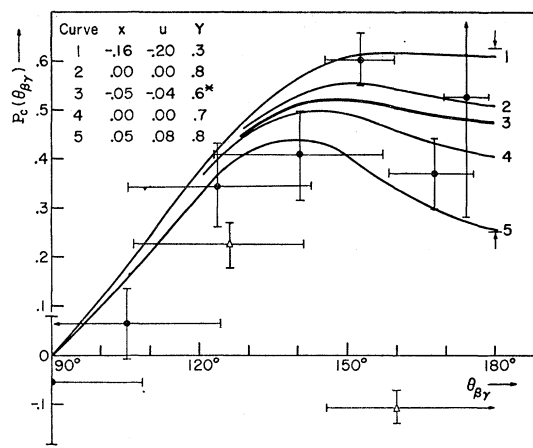


FIG. 7. Experimental  $\text{Sb}^{124}$   $\beta$ - $\gamma$  circular polarization correlation (dots). Also shown are the two points measured by Hartwig and Schopper (triangles). Included are curves for  $P_c(\theta_{\beta\gamma})$  predicted on the basis of various combinations of the matrix elements  $x$ ,  $u$ , and  $Y$ . The arrows indicate the limits acceptable to the computer used in the compilation of the data presented in Table I.

Hartwig and Schopper<sup>18</sup> in that we do not find a change in the sign of  $P_c(\theta_{\beta\gamma})$  as indicated by their data points (see Fig. 7) at  $126^\circ$  and  $160^\circ$ .

### 3. EVALUATION OF EXPERIMENTAL RESULTS

The spin assignment of the  $\beta_1$ - $\gamma$  cascade of  $\text{Sb}^{124}$ , investigated in this paper, is  $3^-(\beta) \rightarrow 2^+(\gamma, E2) \rightarrow 0^+$ . The angular distribution  $P_c(\theta)$  of circularly polarized  $\gamma$  radiation following a first-forbidden  $\beta$  transition is given by Eq. (3). The coefficients  $A_i(W)$  for a  $3^-(\beta^-) \rightarrow 2^+(\gamma, E2) \rightarrow 0^+$  cascade are given by Eqs. (8-10).

In order to determine the combinations of matrix element parameters  $x$ ,  $u$ ,  $Y$ , and  $z$  which satisfactorily fit the experimentally determined  $\beta$ - $\gamma$  circular-polarization correlation, the  $\beta$ - $\gamma$  directional correlation and shape factor of the 2.31-Mev  $\beta$  transition of  $\text{Sb}^{124}$ , the following procedure was adopted.  $C_A \int B_{ij}$  was chosen as the standard matrix element and was set equal to unity (thus  $z=1$ ). Some 125 000 different sets of matrix element parameters  $x$ ,  $u$ , and  $Y$  along with the equations for  $C(W)$ ,  $A_2(W)$ , and  $P_c(\theta)$  were presented to an electronic digital computer.<sup>19</sup> The computer, using only those sets of  $x$ ,  $u$ , and  $Y$  which, within the experimental error, fitted the  $\beta$ - $\gamma$  directional correlation as measured by Steffen,<sup>2</sup> proceeded to compute the shape factor  $C(W)$  and the circular-polarization distribution  $P_c(\theta)$  (at  $W=4.6$ ). The parameters  $x$ ,  $u$ , and  $Y$  were chosen within the limits  $-1 \leq x \leq +1$ ,  $-1 \leq u \leq +1$ , and  $-5 \leq Y \leq +5$ . It is interesting to note that the  $\beta$ - $\gamma$  directional correlation data can be fitted by a wide variety of choices for  $x$ ,  $u$ , and  $Y$ , even though the

<sup>18</sup> G. Hartwig and H. Schopper, Phys. Rev. Letters 4, 293 (1960).

<sup>19</sup> These calculations were performed on the IBM 704 computer of MURA. We are grateful to Mr. Paul Marty and the staff of the MURA computer for making time available to us.

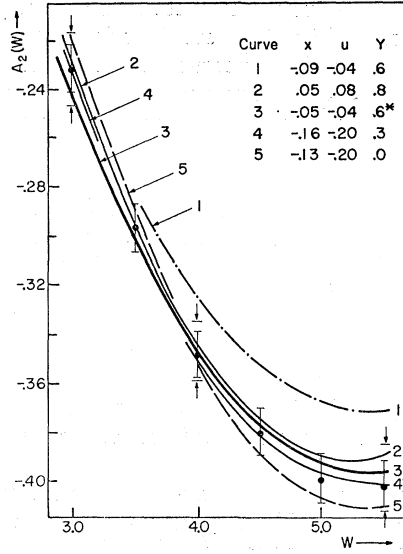


FIG. 8. Some points of the  $\text{Sb}^{124}$   $\beta$ - $\gamma$  directional correlation along with curves predicted on the basis of various combinations of  $x$ ,  $u$ , and  $Y$ . Also indicated (arrows) are the limits imposed on  $A_2(W)$  during the computer compilation of the data presented in Table I.

directional correlation was determined rather precisely over a reasonably large region of  $W$ . Inspection of the computed curves revealed that  $A_2(W)$  is rather sensitive to small changes in  $x$  and  $u$  for a given value of  $Y$ . As indicated in Fig. 8, very different sets of  $x$ ,  $u$ , and  $Y$  give quite satisfactory agreement with the experimental curve for  $A_2(W)$ . Thus we cannot escape the conclusion that  $\beta$ - $\gamma$  directional correlation data alone are of somewhat limited value in the determination of all the matrix elements which contribute to a first-forbidden beta decay.

Figure 7 shows a comparison of the experimental points for  $P_c(\theta)$  with some representative curves for  $P_c(\theta)$  computed with sets  $x$ ,  $u$ , and  $Y$  compatible with the experimental directional correlation. The curves for  $P_c(\theta)$  were corrected for the finite angular resolution of the  $\beta$ - $\gamma$  circular-polarization equipment. The matrix element sets listed in Table I were selected on the basis of the additional requirement that they also fit the experimental shape factor<sup>1</sup> (Fig. 9). These sets now fit all data within experimental error. A somewhat generous summary of the errors involved in the final data in Table I may be given in the following way:

$$\begin{aligned}
 Y &= 0.60 \pm 0.30, \\
 x &= -0.055 \pm 0.105, \\
 u &= -0.060 \pm 0.140.
 \end{aligned}$$

Actually, for a given value of, e.g.,  $Y$ , the errors in  $x$  and  $u$  are much smaller than indicated above. For example, at  $Y=0.60$ ,  $x = -0.045 \pm 0.045$  and  $u = -0.040 \pm 0.060$ .

The  $ft$  value of the 2.31-Mev  $\beta$  transition corrected,

TABLE I. Limits of the nuclear matrix element parameters  $x$ ,  $u$ , and  $Y$  which are consistent with the experimental curves.

$Y$	$x_{\min}$	$x_{\max}$	$u_{\min}$	$u_{\max}$
0.30	-0.160	-0.080	-0.200	-0.080
0.40	-0.130	-0.050	-0.150	-0.050
0.50	-0.110	-0.030	-0.115	-0.010
0.60	-0.085	0.000	-0.095	0.020
0.70	-0.060	0.020	-0.075	0.050
0.80	-0.030	0.050	-0.045	0.080
0.90	-0.005	0.005	-0.020	-0.005

for the nonstatistical shape of the  $\beta$  spectrum, is  $f_{ct} = 4 \times 10^{10}$  sec or  $f_{ct} = 3.1 \times 10^{21}$  in units  $\hbar = m = c = 1$ . From Eq. (6) we obtain for the matrix element parameter of the transition  $|s| = 8.0 \times 10^{-16}$  in units  $\hbar = m = c = 1$ . With this value of  $|s|$  and the parameter values given above we obtain for the nuclear matrix elements<sup>20</sup> [cf. Eq. (5)]:

$$\int B_{ij}/R = \pm (1.4 \pm 0.2) \times 10^{-2},$$

$$\int \mathbf{r}/R = \mp (9.3 \pm 17.6) \times 10^{-4},$$

$$\int (i\boldsymbol{\sigma} \times \mathbf{r})/R = \mp (8.1 \pm 18.9) \times 10^{-4}.$$

The values of these matrix elements, which are of the moment type, are divided by the nuclear radius of

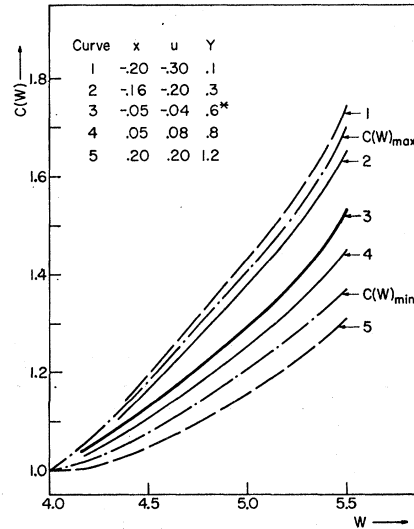


FIG. 9.  $\text{Sb}^{124}$  shape correction factor curves predicted for various combinations of  $x$ ,  $u$ , and  $Y$ . The curves are all normalized to 1.0 at  $W=4.0$ .  $C(W)_{\max}$  and  $C(W)_{\min}$  represent the maximum and minimum values of the normalized shape correction factor as measured by Langer and Smith.

<sup>20</sup> For this computation the following values of the coupling constants were used;  $C_V = g = (1.41 \pm 0.01) \times 10^{-49}$  erg cm<sup>3</sup>, or  $C_V = g = 2.97 \times 10^{-12}$  in units  $\hbar = m = c = 1$ , and  $C_A = -1.20 C_V$ .

Sb<sup>124</sup> ( $R=6.2\times 10^{-12}$  cm,  $R=0.016\hbar/mc$ ) in order to represent them in a manner independent of the units employed.

It is apparent that  $\int \mathbf{r}/R$  and  $\int (i\boldsymbol{\sigma}\times\mathbf{r})/R$  are small compared to  $\int B_{ij}/R$ . If we assume  $\int \mathbf{r}$  and  $\int i\boldsymbol{\sigma}\times\mathbf{r}$  to be zero, we find

$$\int i\boldsymbol{\alpha} = \pm(1.6\pm 0.8)\times 10^{-4}.$$

It may be noted that our data indicate that  $Y\neq 0$  and therefore for  $x=u=0$ ,  $\int i\boldsymbol{\alpha}\neq 0$ . All the experimental data may be satisfactorily represented by

$$\int B_{ij}/R = \pm(1.4\pm 0.2)\times 10^{-2},$$

$$\int \mathbf{r} \simeq 0,$$

$$\int (i\boldsymbol{\sigma}\times\mathbf{r}) \simeq 0,$$

$$\int i\boldsymbol{\alpha} = \pm(1.6\pm 0.8)\times 10^{-4}.$$

In order to extract a more accurate value of  $\int i\boldsymbol{\alpha}$  it will be necessary to make measurements of considerably greater accuracy. The preceding considerations indicate that the significant measurable parameter is  $Y$ , a linear combination of the  $\lambda=1$  type matrix elements, and not the individual matrix elements  $\int i\boldsymbol{\alpha}$ ,  $\int \mathbf{r}$ , and  $\int i\boldsymbol{\sigma}\times\mathbf{r}$ .

#### 4. DISCUSSION

The experimentally determined values of the matrix elements clearly indicate that the deviation from the  $\xi$  approximation of the 2.31-Mev  $\beta$  transition of Sb<sup>124</sup> is due to an inhibition of the  $\lambda=1$  matrix elements  $\int i\boldsymbol{\alpha}$ ,  $\int \mathbf{r}$ , and  $\int i\boldsymbol{\sigma}\times\mathbf{r}$ . Thus this deviation may not be caused by a mutual cancellation of (otherwise large) matrix elements.

The small values of  $\int \mathbf{r}/R$ ,  $\int i\boldsymbol{\sigma}\times\mathbf{r}/R$ , and  $\int i\boldsymbol{\alpha}$  indicate the lack of overlap of the nuclear wave functions which occur in the matrix elements. A perfect overlap of the wave functions of the initial and final nuclear states would result in values of  $\int \mathbf{r}/R$  and  $\int i\boldsymbol{\sigma}\times\mathbf{r}/R$  which are close to unity. The relativistic matrix element  $\int i\boldsymbol{\alpha}$  would then be of order  $v_{\text{nucleon}}/c \simeq 0.1$ . This case of a first-forbidden  $\beta$  transition involving matrix elements with perfectly overlapping wave functions might be called a "superfavored" first-forbidden  $\beta$  transition in analogy to the similar situation with regard to superallowed  $\beta$  transitions. One would expect the  $ft$  values of such transitions to be of the order  $ft \simeq 10^5$  sec. Some such cases of superfavored first-forbidden transitions are known in heavy nuclei, e.g., Pb<sup>210</sup>, Hg<sup>205</sup>, Tl<sup>207</sup>, and

Pb<sup>209</sup>. The  $\beta$  transitions of these nuclei have  $ft$  values ranging from  $10^{5.2}$  to  $10^{5.5}$  sec. It is interesting to note that all  $\lambda=1$  matrix elements involved in the 2.13-Mev  $\beta$  transition of Sb<sup>124</sup> are reduced by a factor roughly of 1000 or more as compared to the ones in superfavored first-forbidden  $\beta$  transitions.

Actually, the  $ft$  values of most nonunique first-forbidden  $\beta$  transitions which do not show large deviations from the  $\xi$  approximation, are of the order  $ft \simeq 10^7$  sec, indicating that the nuclear matrix elements in an ordinary nonunique  $\beta$  transition are about 10 times smaller than would be expected on the basis of a perfect overlap of the initial and final state nuclear wavefunctions. Thus in comparison to "ordinary" nonunique  $\beta$  transitions, the  $\lambda=1$  type matrix elements of the Sb<sup>124</sup> 2.31-Mev transition are reduced by a factor of 100 or more.

The  $ft$  values of unique first-forbidden transitions are of the order  $ft=10^{8.5}$  sec, corresponding to a  $\int B_{ij}$  matrix element of magnitude  $\int B_{ij}/R=0.2$ . Compared to this "normal" value of the tensor-type matrix element, the  $\int B_{ij}$  matrix element contribution to the 2.31-Mev  $\beta$  transition of Sb<sup>124</sup> is reduced by a factor of only about 10. In the case of the Sb<sup>124</sup>  $\beta$  transition this results in a predominance of the tensor component over the much more inhibited  $\lambda=1$  components. The same situation also prevails in the 1.591-Mev  $\beta$  transition of Sb<sup>124</sup> which leads to the second excited state of Te<sup>124</sup>.<sup>21</sup>

The reductions of the  $\beta$ -matrix elements in the Sb<sup>124</sup>  $\beta$  transitions seem to be due to a  $j$ -selection rule effect.<sup>22</sup> In fact, the odd parity of the  $(3^-)$   $_{51}\text{Sb}^{124}$  ground state is probably due to the odd-parity neutron orbital  $h_{11/2}$ . Considering the spin ( $I=7/2$ ) and magnetic moment ( $\mu=+2.55$  nuclear magnetons) of the  $_{51}\text{Sb}^{123}$  ground state, the 51st proton in  $_{51}\text{Sb}^{124}$  is probably in a  $g_{7/2}+$  orbital. The only orbitals available for the proton created in the  $\beta$  decay of  $_{51}\text{Sb}^{124}(3^-)$  to  $_{52}\text{Te}^{124}(2+)$  are the even-parity states  $g_{7/2}+$ ,  $d_{5/2}+$ ,  $d_{3/2}+$ , and possibly  $s_{1/2}+$ . Thus the total angular-momentum change ( $\Delta j$ ) of the nuclear orbitals in the  $n \rightarrow p + \beta^- + \gamma$  transition, must at least be two units. Thus only the tensor component  $\int B_{ij}$  is allowed by the  $\Delta j$  selection rule. Actually the same situation prevails for all first-forbidden transitions as long as the  $n \rightarrow p$  transition involves orbitals within the same major shell.

It is interesting to note that all carefully investigated nonunique first-forbidden transitions with  $\Delta I = \pm 1$  show evidence of a large  $\int B_{ij}$  contribution (e.g., Eu<sup>152</sup>, Eu<sup>154</sup>, Ga<sup>72</sup>, and La<sup>140</sup>).<sup>1,23-26</sup> even though in some of these  $\beta$  transitions (e.g., Eu<sup>152</sup>, Eu<sup>154</sup>, and La<sup>140</sup>) the

<sup>21</sup> H. Paul, Phys. Rev. **121**, 1175 (1961).

<sup>22</sup> R. W. King and D. C. Peaslee, Phys. Rev. **94**, 1284 (1954).

<sup>23</sup> J. W. Sunier, P. Debrunner, and P. Scherrer, Nuclear Phys. **19**, 62 (1960).

<sup>24</sup> S. K. Bhattacharjee and S. K. Mitra, Nuovo cimento **16**, 175 (1960).

<sup>25</sup> R. G. Wilkinson, K. S. R. Sastry, and R. F. Petry, Bull. Am. Phys. Soc. **6**, 72 (1961).

<sup>26</sup> J. E. Alberghini and R. M. Steffen (to be published).

$\Delta j$  selection rule does not seem to be responsible for the large relative  $\mathcal{F}B_{ij}$  component. The absence of any indication of the  $\mathcal{F}B_{ij}$  component in most first-forbidden  $\beta$  transitions with  $\Delta I=0$ , is possibly due to the large contributions of the  $\lambda=0$  matrix elements ( $\int i\gamma_5, \int \sigma \cdot \mathbf{r}$ ).

The considerations presented above are obviously of a qualitative nature only. Even though a large amount of configuration mixing *within* major shells is undoubtedly present in the case of  $\text{Sb}^{124}$ , this does not change the qualitative aspect of the conclusion that the

reduction of the  $\lambda=1$  matrix elements is due to  $\Delta j$  selection rule effects. On the other hand, the fact that a large reduction of the  $\lambda=1$  matrix elements has been established, shows that little or no configuration mixing *outside* major shells is present.

#### ACKNOWLEDGMENTS

The authors wish to convey their appreciation to Professor R. W. King and to Professor H. Paul for a number of useful discussions.

PHYSICAL REVIEW

VOLUME 124, NUMBER 1

OCTOBER 1, 1961

### $L$ to $K$ Ratios in the Electron Capture Decay of $\text{W}^{181}$ and $\text{Ta}^{179\dagger}$

R. C. JOPSON, HANS MARK, C. D. SWIFT, AND J. H. ZENGER

*Lawrence Radiation Laboratory, University of California, Livermore, California*

(Received February 2, 1961)

The  $L$  to  $K$  ratios in the electron capture decay of the isotopes  $\text{Ta}^{179}$  and  $\text{W}^{181}$  have been redetermined. Thin (0.060 in.) NaI crystals with thin (0.002 in.) Be windows were used to detect the  $L$  and  $K$  x rays. The partial fluorescence yields of the  $L$  subshells of Hf and Ta were also measured by determining the coincidence rates between the  $L$  and the  $K$  x rays emitted by the sources. It is necessary to know the fluorescence yields if the  $L$  to  $K$  ratios are to be determined from the measured intensities of the  $L$  and the  $K$  x rays. The  $L$  to  $K$  ratio of  $\text{Ta}^{179}$  was found to be  $0.63 \pm 0.06$ , which implies a total decay energy of approximately  $115 \pm 5$  kev for this isotope. This energy is consistent with the observation that no gamma rays accompany the decay of  $\text{Ta}^{179}$  since the first excited level of  $\text{Hf}^{179}$  has an energy (122 kev) exceeding the total decay energy of  $\text{Ta}^{179}$ . The  $L$  to  $K$  ratio of  $\text{W}^{181}$  was found to be  $0.23 \pm 0.05$ , from which a decay energy of approximately 260 kev is computed. This result is in agreement with the fact that two weak gamma rays are emitted by the source, one at 137 kev and the other at 152 kev. These gamma rays correspond to excited levels in  $\text{Ta}^{181}$ . These gamma rays are in coincidence with the  $L$  x rays emitted by the source but not with the  $K$  x rays, which means that the total decay energy of  $\text{W}^{181}$  must exceed 166 kev. The  $L$  to  $K$  capture ratios reported here are not in good agreement with previously reported values.

#### INTRODUCTION

**W**HENEVER a nucleus is unstable against positron emission, but does not have the decay energy necessary to create the positron, it decays by capturing an orbital electron and emitting a neutrino. The most prominent electromagnetic radiations observed in an electron-capture decay are usually the characteristic x rays of the daughter nucleus. These may be either the  $K$ ,  $L$ , or higher-shell x rays, depending upon which electron is captured in the decay. The relative number of vacancies created in the various atomic sub shells by the decay process depends on the nature of the  $\beta$  decay and on the total energy of the transition.

If the decay energy is very much larger than the electron binding energy in the various sub shells, then, for allowed and first-forbidden transitions, the ratios of  $K$  to  $L$  to  $M$  capture depend only on the electron densities in these shells at the nucleus. On the other hand, if the decay energy is comparable to the binding

energy in the  $K$  shell, then the  $L$  to  $K$  capture ratio is a function of the decay energy, the dependence being such that the emission of high-energy neutrinos is favored.<sup>1</sup> Since no other way exists to determine the decay energy for electron capture processes, it is of some importance to measure the  $L$  to  $K$  capture ratios as accurately as possible.

It is difficult to determine the relative number of  $L$  and  $K$  vacancies from the relative intensities of the  $L$  and  $K$  x rays emitted by the source. In the case of  $K$  capture, most of the  $K$  x rays emitted also create an  $L$ -shell vacancy, and the  $L$  x rays emitted by the filling of these vacancies must somehow be distinguished from  $L$  x rays which follow  $L$ -electron capture. In addition every  $K$  or  $L$  vacancy created does not always result in the emission of the corresponding x ray. The energy of the transition can be dissipated by the emission of one of the outer electrons of the atom. (Electrons resulting from such processes are called Auger electrons.) For the isotopes studied here, this effect was not too important for  $K$  electrons since only about 7% of the

<sup>†</sup> Work done under the auspices of the U. S. Atomic Energy Commission.

<sup>1</sup> R. E. Marshak, Phys. Rev. **61**, 431 (1942).